

Accepted Article

Title: From Discrete Molecular Cage to Networked Cage Exhibiting Enhanced CO₂ Adsorption Capacity

Authors: Lei Zhang, Long Xiang, Cheng Hang, Wenlong Liu, Wei Huang, and YiChang Pan

This manuscript has been accepted after peer review and appears as an Accepted Article online prior to editing, proofing, and formal publication of the final Version of Record (VoR). This work is currently citable by using the Digital Object Identifier (DOI) given below. The VoR will be published online in Early View as soon as possible and may be different to this Accepted Article as a result of editing. Readers should obtain the VoR from the journal website shown below when it is published to ensure accuracy of information. The authors are responsible for the content of this Accepted Article.

To be cited as: *Angew. Chem. Int. Ed.* 10.1002/anie.201702399
Angew. Chem. 10.1002/ange.201702399

Link to VoR: <http://dx.doi.org/10.1002/anie.201702399>
<http://dx.doi.org/10.1002/ange.201702399>

From Discrete Molecular Cage to Networked Cage Exhibiting Enhanced CO₂ Adsorption Capacity

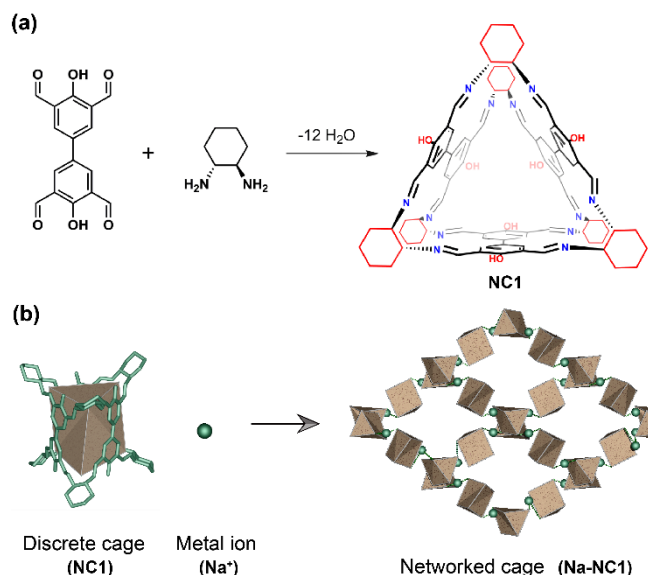
Lei Zhang, Long Xiang, Cheng Hang, Wenlong Liu, Wei Huang* and Yichang Pan*

Abstract: We have adopted the concept of ‘cage to frameworks’ to successfully produce a Na-N connected coordination networked cage Na-NC1 by using a [3+6] porous imine-linked organic cage NC1 (Nanjing Cage 1) as the precursor. It is found that Na-NC1 exhibits hierarchical porosity (inherent permanent voids and interconnected channel) and gas sorption measurements reveal a significantly enhanced CO₂ uptake (1093 cm³ g⁻¹ at 23 bar and 273 K) than that of NC1 (162 cm³ g⁻¹ under the same condition). In addition, Na-NC1 exhibits very low CO₂ adsorption enthalpy making it a good candidate for porous materials with high CO₂ storage and low adsorption enthalpy simultaneously.

Porous materials are important candidates in the applications of gas storage, molecular separation and catalysis. Much efforts have been focused on the ultimate goal of finely controlling the structures and properties of porous materials. Among them, a powerful method, i.e. ‘reticular synthesis’,^[1] has been developed, in which a variety of building blocks (also known as molecular components) are linked to neighboring subunits to construct defined structures. Most extended networks have been readily generated by this method, including metal-organic frameworks (MOFs)^[2] linked by the coordinative bonds and covalent organic frameworks (COFs)^[3] connected by the covalent bonds. A particular advantage of this method is the potential to precisely introduce useful functionalities into the structures by varying the building blocks (metal ions or organic linkers), and the properties of resulting materials can be further tuned by altering the implanted functional groups.^[4]

In contrast to MOFs and COFs with extended networks, porous organic cages (POCs)^[5] are a new class of crystalline materials composed of discrete organic molecules with permanent inherent voids, where the porosity of this type of soluble materials can be

created by cage modules in predictable or ineffective packing ways via weak intermolecular interactions.^[5b,5c,6] For example, Cooper and co-workers have developed some powerful strategies such as ‘mix and match’,^[7] ‘cage scrambling reaction’^[8] and ‘crystal retro-engineering’,^[9] to control over crystal packing and pore connectivity. However, it is still highly challenging to predict the packing modes of small molecules in the crystalline material because small alterations could make a huge impact on the crystal packing in some cases.^[5f,10] Analogous to the construction of MOFs and COFs, the term of ‘reticular synthesis’ may also be applied for building networked cages if discrete organic cages are regarded as the big building blocks. In this respect, Cooper’s^[1] and Zhang’s groups^[12] have reported two instances on porous networked cages containing reduced amine organic cage building blocks. The former was a zinc-mediated cage-MOF connected by the coordinative bonds, and the later was cage-base frameworks linked by covalent bonds. However, they both employed reduced amine cages as the building blocks to constitute cage-extended networks because of the dynamic reversible nature of imine bonds, which led to flexible structure and loss of internal cavities and pores and thus unsuitable for the gas sorption. So an alternative strategy is needed to maintain both the cage shape and inherent void.



Scheme 1. Synthetic route of discrete cage NC1 and networked cage Na-NC1.

Herein, we have adopted the concept of ‘cage to frameworks’^[9] to successfully produce a soluble Na-N connected coordination networked cage Na-NC1 by using a [3+6] porous imine-linked organic cage NC1 as the precursor (Scheme 1). Nevertheless, an

[*] L. Zhang, C. Hang, Prof. W. Huang*
State Key Laboratory of Coordination Chemistry,
School of Chemistry and Chemical Engineering,
Nanjing University,
Nanjing, 210023, P. R. China
E-mail: whuang@nju.edu.cn
L. Xiang, Prof. Y.-C. Pan
State Key Laboratory of Materials-Oriented Chemical Engineering,
College of Chemical Engineering,
Nanjing Tech University,
Nanjing, 210009, P. R. China
E-mail: panyc@njtech.edu.cn
Prof. W.-L. Liu
College of Chemistry and Chemical Engineering,
Yangzhou University,
Yangzhou, 225002, P. R. China

Supporting information for this article is available on the WWW under
<http://dx.doi.org/10.1002/anie.201702399>.

alternative synthetic strategy is adopted by using a rigid imine cage building block instead of the flexible reduced amine form. X-ray single-crystal diffraction analyses of NC1 and Na-NC1 confirm the achievement of our synthetic strategy from a rigid discrete molecular cage to a networked cage and the latter possesses hierarchical porosity (both inherent voids and interconnected channel). More importantly, gas sorption experiments of Na-NC1 exhibit significantly enhanced capacity toward CO₂ at high pressure in comparison with that of NC1 and remarkably low CO₂ adsorption enthalpy for Na-NC1.

The imine-linked cage NC1 was synthesized by a condensation reaction between 3,3',5,5'-tetraformyl-4,4'-biphenyldiol and (1*R*,2*R*)/(1*S*,2*S*)-1,2-diaminocyclohexane in a [3+6] cycloaddition via a 'mix and match' approach (see SI for detailed experimental data). The crystal structure of NC1 shows triangular prism configuration which is similar to that of racemic TCC1 cage without hydroxyl groups both in window size and cage shape.^[13] It is interesting that addition of hydroxyl groups does not lead to a totally different structure, which may allow for the introduction of some other functional groups without altering the [3+6] cage configuration. Different from the MC cages with internal polar cavities,^[14] a distinguishing feature of NC1 is that it bears six terminal hydroxyl groups pointing outside of the cage, which may provide available sites for further outer post-modification.^[15] Two different types of imine units can be found in the molecular structure of NC1. One is involved in the hydrogen bond with an adjacent hydroxyl group whereas the other does not. This discrepancy could be further supported by the ¹³C NMR spectra (see SI Section S2). In the crystal stacking of NC1, neighboring cages adopt the columnar packing with a bite angle of 60° (Figure S16), which is analogous to the so-called window-to-window crystal stacking fashion^[7] originated from the chiral interactions between two opposite enantiomers via the 'mix and match' strategy. Thus, interconnected one-dimensional (1D) tubular channel is generated running through the intrinsic cage voids, which is similar to that observed in NDI-Δ^[16] and racemic TCC1 cage (Figures S15-16).

Na-NC1 was synthesized by adding excess NaN₃ into the *N,N*-dimethylformamide/1,4-dioxane mixture of [3+6] imine cage (see SI for detailed experimental data), and the crystalline solid of Na-NC1 was collected from the mother solution by slow evaporation in air for 3 weeks. It should be mentioned that Na-NC1 has good solubility in common organic solvents, and the ¹H NMR spectra of Na-NC1 showed distinct signals compared to that of NC1 (Figures S1, S4), especially for the phenyl and imine protons. X-ray single-crystal diffraction analysis of Na-NC1 indicates that three types of crystallographically independent Na(I) centers are present. All Na(I) ions are three-coordinated by one oxygen atom and two imine nitrogen atoms from neighboring cages, as shown in Figure 1a. Among them, Na(1) and Na(2) are bridged by one hydroxyl group and Na(3) is coordinated by an ending water molecule. As a result, a 1D single-strand helices are formed along *c* axis (Figure 1b) via the Na-N coordinative bonds in the lengths of 2.935(5), 2.998(6) and 2.877(6) Å, and the pitch length of every helical cycle is 38.917(5) Å. The 1D helices are further fabricated into a three-dimensional (3D) porous network by van der Waals interactions (Figures 1e, S17), in which uniform channels are formed along different axial directions and [111] plane (Figures 1c, S18). Actually, it is found that Na-NC1 has a hierarchically porous structure composed of inherent permanent cavities and interconnected channel (Figure 1d). In addition, the

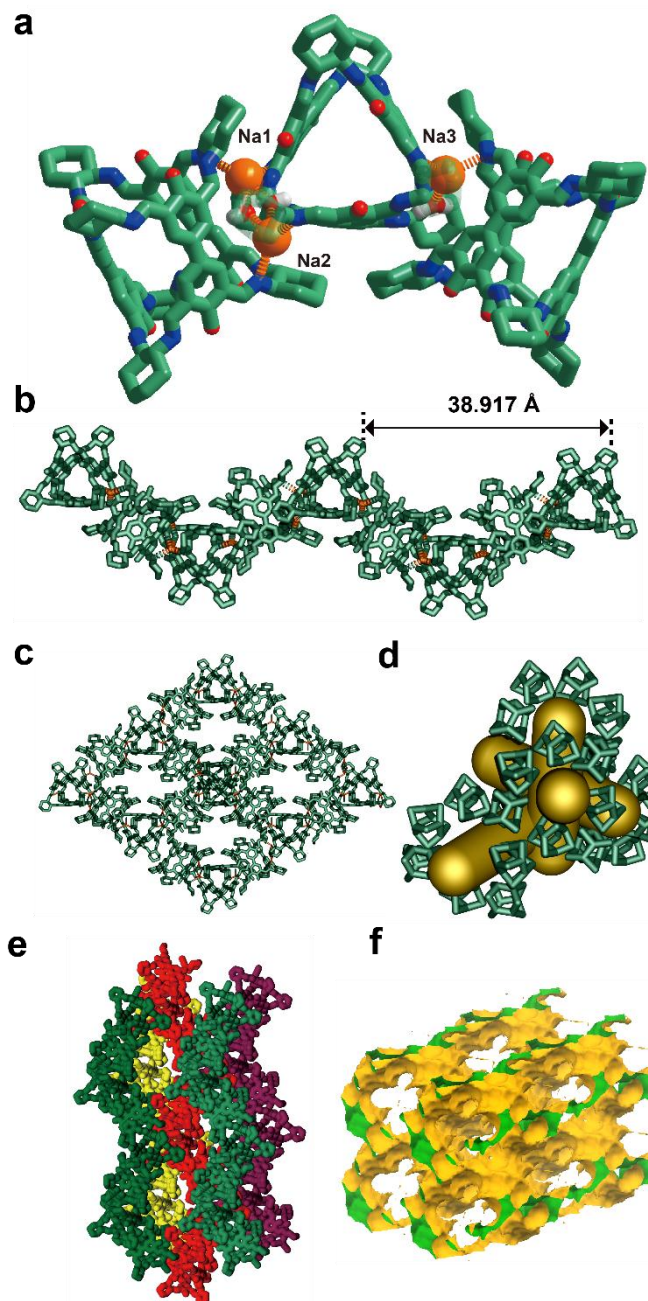


Figure 1. Crystal structure of Na-NC1: (a) Coordination environments for three kinds of sodium ions; (b) 1D single-strand helices along *c* axis connected by the Na-N coordinative bonds; (c) Interconnected channel viewed along *b* axis; (d) Schematic representation of hierarchical porosity composed of cage cavity and interconnected channel; (e) Space-filling representation of the 3D structure composed of single-strand helices; (f) Solvent-accessible surface diagram using a probe radius of 1.82 Å (2×2×2 supercell), green: inside surface, yellow: outside surface.

solvent accessible surface for N₂ probe radius also shows interconnected channel (Figure 1f). Owing to the hierarchical porosity of Na-NC1, the density of the solvent-free crystal of Na-NC1 (0.637 g cm⁻³) is 62.3% of that of NC1, and the percentage of the total potential solvent accessible volume of Na-NC1 (56.3% calculated by Platon) is 2.2 times as that of NC1.

By comparing the structures of NC1 and Na-NC1, the above-mentioned hydrogen bonding interactions between the hydroxyl and imine groups are both observed before and after Na(I) ion complexation. It is suggested that this type of strong O-H...N

hydrogen bonds may prevent the deformation or destruction of imine-linked cage building blocks during the coordination process. On the other hand, the selection of a monocovalent alkali metal Na(I) ion with weak coordination ability could minimize the number of guest counterions and the influence of dynamic reversibility of imine bonds. In addition, it is already known to us that the O-H...N hydrogen bonding interactions may help to improve crystallinity of the cages.^[17] So the reduced amine cage is unnecessary for the formation of our unique sodium-directed networked cage.

NC1 and Na-NC1 can be desolvated by using super-critical carbon dioxide activation to yield guest-free porous solids for adsorption-desorption measurements (See SI Section S4). NC1 shows type I N₂ sorption behavior with a corresponding BET surface area of 802 m² g⁻¹ (Langmuir surface area 891 m² g⁻¹) at 77 K (Figure 2a), which is close to that of the racemic cage TCC1^[13] (881 m² g⁻¹). In contrast, Na-NC1 displays non-porous towards N₂ at 77 K, which may be attributed to two possible reasons. One is N₂ is a diatomic molecule with a quadrupole moment which produces specific interactions at the gas-solid interface, and the other is that N₂ molecules may have a diffusion problem within the pores at 77 K.^[18] As an alternate, argon is used as the probe molecule to obtain the sorption-desorption isotherm, and Na-NC1 exhibits a type I Ar adsorption isotherm with a BET surface area of 1230 m² g⁻¹ (Langmuir surface area 1670 m² g⁻¹) at 87 K (Figure 2b). This value could be also supported by CO₂ adsorption isotherm at 196 K, where similar BET surface areas of 1219 and 1218 m² g⁻¹ are obtained by using BET and *t*-plot methods, respectively (see Section S6). The experimental BET surface area of Na-NC1 is lower than its simulated one at 1741 m² g⁻¹ (See Section S6). The total pore volume of Na-NC1 is 0.78 cm³ g⁻¹ according to the Ar adsorption isotherm at 87 K. Pore size distribution calculated by non-local density functional theory from Ar sorption analyses for Na-NC1 (Figure S19) reveals the presence of pores with different size (5.0, 5.8, 6.5 Å). The results indicate that Na-NC1 has a hierarchically porous structure, which is consistent with its crystal structure (Figure S18).

CO₂ sorption at 273 and 298 K at high pressure (up to 30 bar) has been carried out for desolvated cages NC1 and Na-NC1. CO₂ sorption isotherms for crystalline Na-NC1 exhibit type II behavior without the hysteresis on adsorption and desorption isotherms, indicating that CO₂ favors multi-layer adsorption on surface of Na-NC1 at high pressure (Figure 2c). Interestingly, Na-NC1 absorbs a significantly large amount of CO₂ up to 1093 cm³ (STP) g⁻¹ (68.2 wt%) at 23 bar and 273 K, which is much higher than NC1 (162 cm³ g⁻¹ under the same experimental condition) and all the previously reported imine-based cages (Table S2). Accordingly, Na-NC1 takes up a moderate amount of CO₂ (790 cm³ g⁻¹) at 30 bar and 298 K. As far as we are aware, networked cage Na-NC1 exhibits competitive CO₂ storage capacity given the low surface areas and small pore volume, in contrast to some other porous materials including MOFs, COFs and organic polymers,^[19] as listed in Table S2.

Moreover, isosteric heat of CO₂ adsorption (*Q*_{st}) for both materials has been calculated by Clausius-Clapeyron equation (Figure 2d and SI Section S5) from their adsorption isotherms at 273 and 298 K. As illustrated in Figure 2d, the *Q*_{st} value for NC1 (black line) decreases continuously from 18.0 to 12.0 KJ mol⁻¹ with the CO₂ uptakes in the range 0-1.8 mmol g⁻¹, and then it increases to 16.0 KJ mol⁻¹ at 3.4 mmol g⁻¹. In contrast, the *Q*_{st}

value for Na-NC1 falls within a broader range 4.7-20.4 KJ mol⁻¹ (red line in Figure 2d), accompanied by high CO₂ uptakes up to 38.5 mmol g⁻¹, where a sharp decrease from 20.4 to 4.7 KJ mol⁻¹ is found in the range 0-10 mmol g⁻¹ and a slightly increased process for the *Q*_{st} value is followed until 38.5 mmol g⁻¹. It should be pointed out that the lowest *Q*_{st} value of Na-NC1 corresponds to a CO₂ uptake of ~10 mmol, which agrees well with the CO₂ monolayer adsorption capacity of 9.4 mmol g⁻¹ calculated from its CO₂ adsorption isotherm at 196 K by using BET modes (Figure S29). The continuous decrease of *Q*_{st} values and the match of CO₂ uptake at the lowest *Q*_{st} with monolayer adsorption capacity both imply that the first layer of CO₂ adsorbed on the surface of Na-NC1 dominates the adsorption process when the CO₂ loading is less than ~10 mmol g⁻¹, and Na-NC1 possesses heterogeneous binding sites with CO₂.^[20] Actually, the isosteric heat of CO₂ adsorption for Na-NC1 is very low in comparison with other sort of porous materials with high CO₂ adsorption capacity (Table S2), indicative of weak physisorption with CO₂ rather than chemisorption. As we know, most porous materials with high CO₂ adsorption have relative high adsorption enthalpy leading to high desorption temperature, and thus high costs of regeneration are accompanied. So our networked cage Na-NC1 is suggested to be a candidate for CO₂ storage since it meets the long-sought requirements for porous materials with high CO₂ storage and low adsorption enthalpy simultaneously.

In order to further verify the reason why Na-NC1 has an enhanced CO₂ uptake, control experiments have been performed to compare the CO₂ sorption capacity for amorphous and crystalline Na-NC1 and NC1 (Figures S12, S21). Amorphous solid of Na-NC1 and NC1 has been prepared via freeze-drying from their CHCl₃ solutions (see Section S1). The results indicate that both of amorphous samples have low CO₂ uptakes less than ~90 cm³ g⁻¹ at 30 bar and 298 K, clearly manifesting the "loss" of enhanced CO₂ adsorption ability for amorphous Na-NC1. So the formation of unique interconnected channels observed in the crystal packing of hierarchically porous structure plays a vital role in enhanced CO₂ adsorption capacity of Na-NC1. In addition, volumetric CH₄, N₂ and H₂ uptakes for NC1 and Na-NC1 have been measured for comparisons. The results reveal that both materials adsorb little CH₄ and N₂ at 298 K compared with CC (Figure S20), and the CO₂/N₂ selectivity for Na-NC1 is calculated to be 44 with a capacity of ~4.7 mmol g⁻¹ of CO₂ for CO₂/N₂:10/90 mixture at 10 bar and 273 K (Figure S28) via Ideal Adsorbed Solution Theory (IAST). H₂ sorption measurements for Na-NC1 and NC1 show that the former adsorbs a maximum of 170 cm³ g⁻¹ (7.59 mmol g⁻¹) H₂ at 351 mmHg and 77 K, outperforming 89 cm³ g⁻¹ (3.97 mmol g⁻¹) for the latter (Figure S22). It is worth noting that both Na-NC1 and NC1 maintain good crystallinity before and after the desolvation and gas adsorption experiments (Figures S10-11). Moreover, both NC1 and Na-NC1 show good hydrolytic stability, which can be evidenced by the consistent powder X-Ray diffraction patterns before and after their immersion in pure water up to 10 days (Figures S13-14).

In summary, we have successfully produced a sodium-directed networked cage (Na-NC1) from a rigid imine-linked [3+6] cage (NC1). Na-NC1 has a hierarchically porous structure containing inherent permanent cavities and large interconnected channels. More interestingly, Na-NC1 offers the advantage of excellent CO₂ storage capacity along with low adsorption enthalpy compared to the discrete cage precursor, which may make it very promising materials for CO₂ storage. Both of NC1 and Na-NC1 exhibit good hydrolytic stability. It is believed that the current work provides a feasible method to construct hierarchically porous structures from discrete shape-persistent

porous organic cages. It is also an extension of reticular chemistry by linking complicated and preporous building blocks into infinite frameworks.

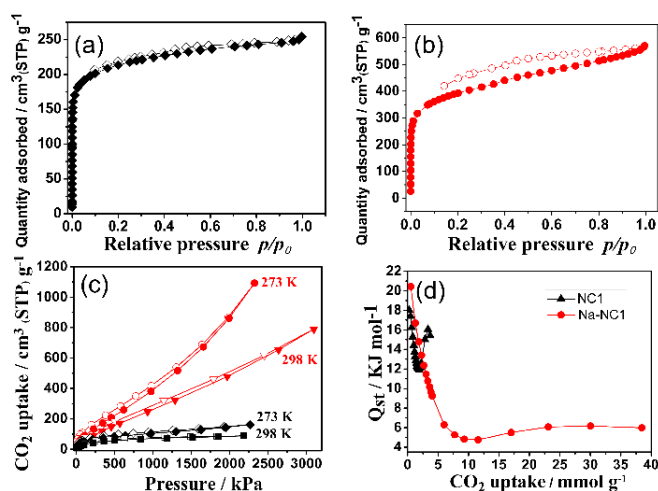


Figure 2. (a) N₂ adsorption and desorption isotherms measured at 77 K for NC1; (b) Ar adsorption and desorption isotherms measured at 87 K for Na-NC1; (c) CO₂ uptakes at 298 and 273 K for Na-NC1 and NC1; (d) Isothermic heat of CO₂ adsorption (Q_{st}) for Na-NC1 and NC1. Red dots and lines represent Na-NC1 and black ones represent NC1.

Acknowledgements

This work was financially supported by the Major State Basic Research Development Programs (No. 2013CB922101), the National Natural Science Foundation of China (No. 21171088), and the project of scientific and technological support program in Jiangsu province (No. BE2014147-2). Special thanks are given to Prof. Xin Zhao in Shanghai Institute of Organic Chemistry, Chinese Academy of Science for his kind assistance with simulated calculations.

Received: ((will be filled in by the editorial staff))

Published online on ((will be filled in by the editorial staff))

Keywords: cage compounds • Schiff bases • hierarchically porous materials • carbon dioxide storage

- [1] (a) O. M. Yaghi, *J. Am. Chem. Soc.* **2016**, 138, 15507-15509; (b) M. Yaghi, M. O'Keeffe, N. W. Ockwig, H. K. Chae, M. Eddaoudi, J. Kim, *Nature* **2003**, 423, 705-714; (c) J. Jiang, Y. Zhao, O. M. Yaghi, *J. Am. Chem. Soc.* **2016**, 138, 3255-3265.
- [2] (a) A. Schoedel, M. Li, D. Li, M. O'Keeffe, O. M. Yaghi, *Chem. Rev.* **2016**, 116, 12466-12535; (b) M. O'Keeffe, O. M. Yaghi, *Chem. Rev.* **2012**, 112, 675-702; (c) H. Li, M. Eddaoudi, T. L. Groy, O. M. Yaghi, *J. Am. Chem. Soc.* **1998**, 120, 8571-8572.

- [3] (a) J. L. Segura, M. J. Mancheno, F. Zamora, *Chem. Soc. Rev.* **2016**, 45, 5635-5671; (b) A. P. Côté, A. I. Benin, N. W. Ockwig, M. O'Keeffe, A. J. Matzger, O. M. Yaghi, *Science* **2005**, 310, 1166-1170; (c) H. M. El-Kaderi, J. R. Hunt, J. L. Mendoza-Cortés, A. P. Côté, R. E. Taylor, M. O'Keeffe, O. M. Yaghi, *Science* **2007**, 316, 268-272.
- [4] X. Kong, H. Deng, F. Yan, J. Kim, J. A. Swisher, B. Smit, O. M. Yaghi, J. A. Reimer, *Science* **2013**, 341, 882-885.
- [5] (a) T. Hasell, A. I. Cooper, *Nat. Rev. Mater.* **2016**, 1, 16053; (b) M. Mastalerz, *Angew. Chem., Int. Ed.* **2010**, 49, 5042-5053; (c) J. R. Holst, A. Trewin, A. I. Cooper, *Nat. Chem.* **2010**, 2, 915-920; (d) T. Tozawa, J. T. A. Jones, S. I. Swamy, S. Jiang, D. J. Adams, S. Shakespeare, R. Clowes, D. Bradshaw, T. Hasell, S. Y. Chong, C. Tang, S. Thompson, J. Parker, A. Trewin, J. Bacsá, A. M. Z. Slawin, A. Steiner, A. I. Cooper, *Nat. Mater.* **2009**, 8, 973-978; (e) A. I. Cooper, *Angew. Chem., Int. Ed.* **2011**, 50, 996-998; (f) M. W. Schneider, I. M. Oppel, H. Ott, L. G. Lechner, H.-J. S. Hauswald, R. Stoll, M. Mastalerz, *Chem. – Eur. J.* **2012**, 18, 836-847; (g) Wang, C. Zhang, B. C. Noll, H. Long, Y. Jin, W. Zhang, *Angew. Chem., Int. Ed.* **2014**, 53, 10663-10667.
- [6] T. Tozawa, S. Swamy, S. Jiang, D. J. Adams, S. Shakespeare, J. T. A. Jones, R. Clowes, D. Bradshaw, T. Hasell, J. Bacsá, A. Trewin, A. M. Slawin, A. Steiner, A. I. Cooper, *Nat. Mater.* **2009**, 8, 973.
- [7] T. Hasell, S. Y. Chong, K. E. Jelfs, D. J. Adams, A. I. Cooper, *J. Am. Chem. Soc.* **2012**, 134, 588-598.
- [8] S. Jiang, J. T. A. Jones, T. Hasell, C. E. Blythe, D. J. Adams, A. Trewin, A. Cooper, *Nat. Commun.* **2011**, 2, 207.
- [9] M. A. Little, M. E. Briggs, T. A. Jones, M. Schmidtman, T. Hasell, Y. Chong, K. E. Jelfs, L. Chen, A. I. Cooper, *Nat. Chem.* **2015**, 7, 153-159.
- [10] (a) L. A. Stevens, K. P. Goetz, A. Fonari, Y. Shu, R. M. Williamson, J.-I. Brédas, V. Coropceanu, O. D. Jurchescu, G. E. Collis, *Chem. Mater.* **2011**, 23, 112-118; (b) M. A. Little, S. Y. Chong, M. Schmidtman, T. Hasell, A. Cooper, *Chem. Commun.* **2014**, 50, 9465-9468.
- [11] S. I. Swamy, J. Bacsá, J. T. A. Jones, K. C. Stylianou, A. Steiner, L. F. Ritchie, T. Hasell, J. A. Gould, A. Laybourn, Y. Z. Khimyak, D. J. Adams, I. J. Rosseinsky, A. I. Cooper, *J. Am. Chem. Soc.* **2010**, 132, 12773-12775.
- [12] (a) Y. Jin, B. A. Voss, A. Jin, H. Long, R. D. Noble, W. Zhang, *J. Am. Chem. Soc.* **2011**, 133, 6650-6658; (b) Y. Jin, B. A. Voss, R. McCaffrey, C. T. Baggett, R. D. Noble, W. Zhang, *Chem. Sci.* **2012**, 3, 874-877.
- [13] A. G. Slater, M. A. Little, A. Pulido, S. Y. Chong, D. Holden, L. Chen, C. Morgan, X. Wu, G. Cheng, R. Clowes, M. E. Briggs, T. Hasell, K. E. Jelfs, G. M. Day, A. I. Cooper, *Nat. Chem.* **2017**, 9, 17-25.
- [14] M. W. Schneider, I. M. Oppel, A. Griffin, M. Mastalerz, *Angew. Chem., Int. Ed.* **2013**, 52, 3611-3615.
- [15] J. Guo, B. L. Tardy, A. J. Christofferson, Y. Dai, J. J. Richardson, W. Zhu, M. Hu, Y. Ju, J. Cui, R. R. Dagastine, I. Yarovsky, F. Caruso, *Nanotechnol.* **2016**, 11, 1105-1111.
- [16] Z. Liu, G. Liu, Y. Wu, D. Cao, J. Sun, S. T. Schneebeli, M. S. Nassar, C. J. Mirkin, J. F. Stoddart, *J. Am. Chem. Soc.* **2014**, 136, 16651-16660.
- [17] X. Chen, M. Addicoat, E. Jin, L. Zhai, H. Xu, N. Huang, Z. Guo, L. Liu, S. Irlé, D. Jiang, *J. Am. Chem. Soc.* **2015**, 137, 3241-3247.
- [18] (a) F. Rodríguez-Reinoso, J. de D. López-González, C. Berenguer, *Carbon* **1982**, 20, 513-518; (b) J. Silvestre-Albero, A. Silvestre-Albero, F. Rodríguez-Reinoso, M. Thommes, *Carbon* **2012**, 50, 3128-3133; (c) Garrido, A. Linares-Solano, J. M. Martín-Martínez, M. Molina-Sabio, F. Rodríguez-Reinoso, R. Torregrosa, *Langmuir* **1987**, 3, 76-81; (d) T. Nguyen, S. K. Bhatia, *Langmuir* **2008**, 24, 146-154; (e) S.-T. Zheng, J. Bu, T. Wu, C. Chou, P. Feng, X. Bu, *Angew. Chem., Int. Ed.* **2011**, 50, 8858-8862; (f) L. Xu, Y.-P. Luo, L. Sun, Y. Xu, Z.-S. Cai, M. Fang, R.-Y. Yuan, H.-B. Du, *Chem. – Eur. J.* **2016**, 22, 6268-6276.
- [19] D. Yuan, W. Lu, D. Zhao, H.-C. Zhou, *Adv. Mater.* **2011**, 23, 3723-3725.
- [20] (a) A. Khelifa, L. Benchehida, Z. Derriche, *J. Colloid. Interface. Sci.* **2004**, 278, 9-17; (b) A. Khelifa, Z. Derriche, A. Bengueddach, *Microporous Mesoporous Mater.* **1999**, 32, 199-209.

Entry for the Table of Contents

Layout 1:

Anode materials

Lei Zhang, Long Xiang, Cheng Hang,
Wenlong Liu, Wei Huang* and Yichang
Pan* _____ Page 1– Page 4

**From Discrete Molecular Cage to
Networked Cage Exhibiting Enhanced
CO₂ Adsorption Capacity**